www.amlett.com, DOI: 10.5185/amlett.2010.9159 Published online by the VBRI press in 2010

Structural, dielectric and ferroelectric properties of Y^{3+} doped PZT (65/35)

K. L. Yadav[a]*

Ferroic Physics Group, National Institute for Materials Science, Tsukuba, 305-0047 Ibaraki, Japan

[a]Permanent Address. Smart Materials Research Laboratory, Department of physics, Indian Institute of Technology Roorkee, Roorkee 247667, India

*Corresponding author. Tel/Fax: (+91) 1332 285670; E-mail: klyadav35@yahoo.com

Received: 6 Sept 2010, Revised: 24 Sept 2010 and Accepted: 26 Sept 2010

ABSTRACT

Yttrium doped lead zirconium titanate (PYZT) was prepared by chemical co-precipitation technique using their nitrate salts. X-ray diffraction analysis was carried out to confirm the phase formation and to study the structural changes with *Y* doping in PZT. Scanning electron micrographs of the sample show uniform grain distribution with decreasing grain size with *Y* doping. The dielectric maxima was found to be enormously increased from 1791 to 2687 along with decreasing phase transition temperature from 335 to 400 ^{o}C with *Y* doping in PZT. The remnant polarization was also found to increase from ~11 to ~44 μC/cm^2 with *Y* doping.

Keywords: Yttrium doped lead zirconium titanate; co-precipitation technique; dielectric and ferroelectric properties.

K. L. Yadav is currently Associate Professor in the Department of Physics, Indian Institute of Technology Roorkee, India. He is born and brought at Kharagpur, West Bengal, India and hold M.Sc. and Ph.D. degree in Physics from Indian Institute of Technology Kharagpur, India in 1989 and 1994, respectively. In 2001, he became BOYSCAST Fellow at Materials Research Institute, Pennstate University, USA. In addition, he obtained JSPS fellowship at National Institute for Materials Science, Tsukuba, Japan in 2010. In his academic carrier, he has published more than 70 papers in SCI Journals and is an author of one contributory chapter in a book of International level in the field of materials science and technology. His major research interests are Functional Nanomaterials, Mulitferroics, Sensors and Biomaterials. His recent research interest is focused on designing and development of the smart materials for device applications. Dr. Yadav strongly advocates the use of research methodology in the education.

Introduction

$Pb(Zr_xTi_{1-x})O_3$ (PZT), a solid solution of $PbZrO_3$ (PZ) and $PbTiO_3$ (PT) posses perovskite-type ABO_3 structure, with high piezoelectric and dielectric constant (piezoelectric constant d_{33} 150–250 mm/V; dielectric constant at room temperature 500–700) [**1**]. The dielectric characteristics of PZT change with its stoichiometry. Dai et al. [**2**] reported an enhancement in dielectric constant from 10000 to 14000 in PZT, with change in Zr/Ti ratio from 95/5 to 55/45 also the Curie temperature changed from 250 to 380°C. However, the best dielectric and piezoelectric properties of PZT have been found near MPB [**3**]. Due to these technically sound properties of PZT, it has many potential applications in electronic devices, such as nonvolatile memories, infrared sensors, optical shutters, modulators etc [**4-6**]. PZT is most sensitive material to the doping. Its properties can be manipulated by adding foreign ions in the host lattice. A trivalent ion doped at *A* site of ABO_3 acts as donar and reduces the concentration of intrinsic oxygen vacancy created due to PbO evaporation and compensate the hole formed due to lead vacancies, which in tern increases bulk resistance of sample. PZT doped with La^{3+} has been extensively studied and is shown to be useful in many applications such as memories (DRAM and FRAM), infrared detectors, electro-optic devices and surface acoustic wave devices and so forth [**7**]. No systematic work on Y^{3+} doped PZT ceramics was found to the best of author's knowledge. Yttrium by itself does not seem to be

really promising because of relatively lower polarization and dielectric constant values. But due to the large size difference between the available Pb^{2+} size and Y^{3+} cation size, Y^{3+} (r_9^{3+} = 1.075 Å) compared to that of Pb^{2+} (r_{12}^{2+} = 1.49 Å) ion, it is expected to create a distortion in the cell and thereby influence the ferroelectric properties. The possible influence of Y^{3+} addition to the Pb^{2+} site is shown in the following equation: $Y_2O_3 + V_o^{\bullet\bullet} + 2PbO \rightarrow 2Y_{Pb}^{\bullet} + 3O_o^x$. Substitution of Pb^{2+} by Y^{3+} may improve the ferroelectric properties of the PZT by reducing the oxygen vacancy concentration. Hence in the present work we have substituted Y^{3+} ion in place of Pb^{2+} ion of PZT, and systematically studied the effect of doping on structural, dielectric and ferroelectric properties of PZT.

Experimental

Powder samples of the PYZT system were prepared according to the formula $Pb_{1-x}\ Y_x(Zr_{0.65}Ti_{0.35})\ O_3$ via the chemical route for x = 0, 0.02, 0.04, 0.06, 0.08, 0.10. Nitrate salts (AR grade) of component atoms $Pb(NO_3)_2$ (lead nitrate), $Y(NO_3)_3{\cdot}6H_2O$ (yttrium nitrate) and $ZrO(NO_3)_2{\cdot}2H_2O$ (zirconyl nitrate) were dissolved in double distilled water. The resulting solution was stirred on a magnetic stirrer for 2–3 h in order to get a clear transparent solution. Titanium isopropoxide ($C_{12}H_{28}O_4Ti$) was added drop-wise to this solution. The added titanium isopropoxide hydrolysed into an intermediate $Ti(OH)_4$ and slowly redissolved. A few drops of nitric acid were added to dissolve $Ti(OH)_4$ completely and to get a clear solution. A white precipitate was observed immediately after adding some amount of ammonia into the solution. To obtain the desired powder, the solution was vacuum filtered and washed several times with distilled water. The filtered powder cake was then kept in an oven (for 24 h) at 150˚C for drying. Thermal behavior of as dried powder was analyzed using differential thermal analysis (DTA) and thermo gravimetric analysis (TGA), at a heating rate of 10 ^{0}C/min, the oven-dried powder of x = 0.00 composition was calcined at various temperatures 200-100-750 ^{o}C to find the complete phase formation. Then the different compositions of PYZT were calcined at 800 ^{o}C for 4 h. These powders were cold pressed into discs (pellets) at a pressure of 31 MPa using a uniaxial hydraulic press. The pellets were sintered at 1050 ^{o}C for 2 h. The formation and quality of compounds were checked by XRD technique. The X-ray diffraction pattern of the compounds was recorded at room temperature using X-ray powder diffractometer (Brueker D8 Advance) with Cu K_α radiation (1.5418 A°) in a wide range of Bragg angles 2θ (20 - 60^o) at a scanning rate of 2^o per minute. The microstructure and the composition analysis were investigated using a using a field emission scanning electron microscope with energy dispersion X-ray spectroscope attached (Quanta 200). The composition analysis was carried at different spots on the samples by applying accelerating potential of 20 kV. The flat polished surface of sintered pellets were electrode with air drying silver paste and oven dried at 100 ^{o}C for 30 min before taking electrical and dielectrics measurements The dielectric constant (ε) and loss tangent (tan δ) of the compounds were measured using an automated HIOKI 3532-50 Hi Tester, LCR Meter as a function of frequency (100 Hz – 1 MHz) in the temperature range 50 – 300 ^{o}C. Polarization versus electric field (P–E) hysteresis loops were measured at room temperature by modified Sawyer-Tower circuit (Automatic PE loop tracer system).

Results and discussion

Thermal analysis

The DTA and TG curve of the PZT precursors prepared via co-precipitation route is shown in the **Fig. 1**. The minor weight loss at low temperature (less than 150 ^{o}C) is due to the liberation of surface absorbed or occluded solvents, another minor weight loss around 300 ^{o}C is ascribed to the decomposition of complex hydroxides. The major two peak in DTA curve around 428 and 460 ^{o}C along with high weight loss of 16% in TG curve is attributed to the decomposition of lead nitrate $Pb(NO_3)_2$ into PbO [**8**]. The TG curve becomes almost constant after 500 ^{o}C, which gives information about the complete decomposition of complex oxyhydroxides at this temperature and also confirms that this temperature is sufficient to obtain the desired powder through this process. A small exothermic peak at the temperature range of 720 °C, which have no associated weight loss manifestation in the TG curves, may be attributed to the crystallization of perovskite PZT phase. This observation is also confirmed from XRD analysis.

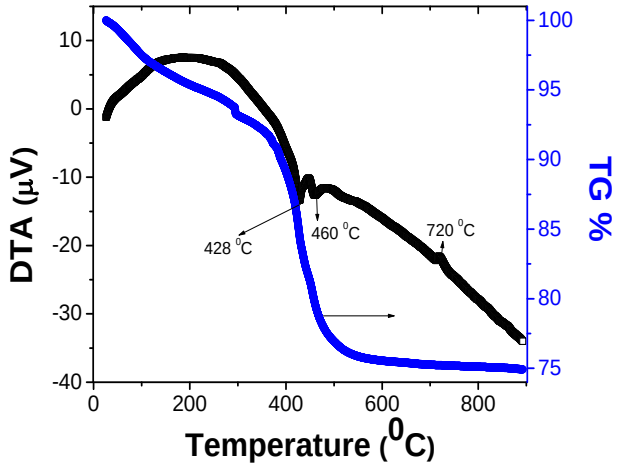

Fig. 1. DTA/TG curve of oven dried powder of PZT (65/35).

Structural analysis

Fig. 2 compares the XRD pattern of the different calcined powders of PZT composition with that of its starting mixture. In the XRD pattern of 200 ^{o}C calcined powder, lead nitrate peaks were found to dominate and are indexed from JCPDS-15, these diffraction peaks of the lead nitrate became significantly weak and broadened when the calcination temperature is increased, In the XRD pattern of 400 ^{0}C calcined powder lead nitrate peaks completely diminish, further few more small peaks of zirconyl nitrate were observed and are marked in **Fig. 2**. Further as the calcination temperature is increased the intensity of the new

set of peaks at $2\theta \approx 31.05$ was found to increase, which can be attributed to a new phase formation during calcination of mixtures. The XRD pattern of 600 ^{o}C calcined powder shows few impure peaks along with perovskite phase peaks, finally the XRD pattern of 750 ^{o}C calcined sample clearly show the formation of single phase, which was identified to be rhombohedral phase from the previous literature [**9**] and the peaks were indexed from it.

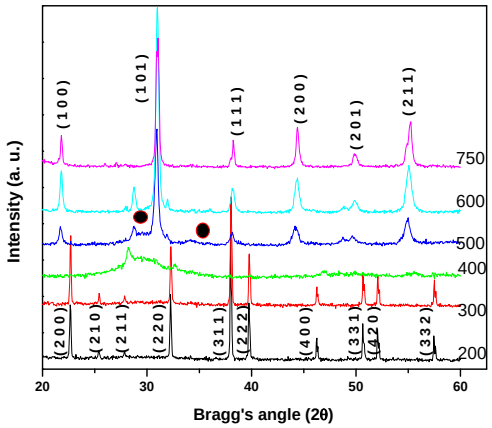

Fig. 2. X-ray diffraction patterns of PYZT, x = 0.00 composition calcined at various temperatures.

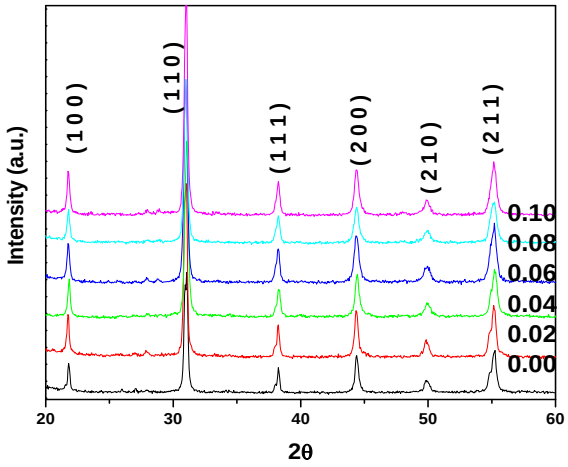

Fig. 3. X-ray diffraction patterns of different *Y* doped PZT (65/35) compositions.

Fig. 3 show the X-ray diffraction pattern of the whole series of sintered samples, all the diffraction peaks corresponds to that of PZT (65/35) rhombohedral structure and no extra peaks, in the range of our experimental errors were observed. Further no sign of change in the peak position or peak splitting was found with yttrium doping upto x = 0.10. The indexing of XRD peaks and determination of lattice parameters of PYZT was carried out using software package, X'pert-plus. On the basis of the best agreement between observed and calculated *d* values of all the reflections, a unit cell of PYZT was selected and its lattice parameters were also refined. The refined lattice parameters are given in **Table 1**. From these data, it is clear that the structure of the phase formed is unchanged, within the composition range studied. The lattice parameter *a* was found to decrease with Y^{3+} doping, which may be due to smaller ionic radii of Y^{3+} (r_9^{3+} = 1.075 Å) compared to that of Pb^{2+} (r_{12}^{2+} = 1.49 Å) ion.

Table 1. Unit cell parameters, grain size and % of porosity variation as function of *Y* doping in PZT (65/35).

Y in PZT(65/35)	Unit cell parameter *a* (Å)	Unit cell parameter *α* (degree)	Grain size (μm)	% of porosity
0.00	4.082	90.075	1.252	3.012
0.02	4.083	90.105	1.293	5.027
0.04	4.083	90.111	1.120	6.323
0.06	4.080	90.130	0.692	6.895
0.08	4.077	90.137	0.572	7.027
0.10	4.075	90.144	0.643	6.817

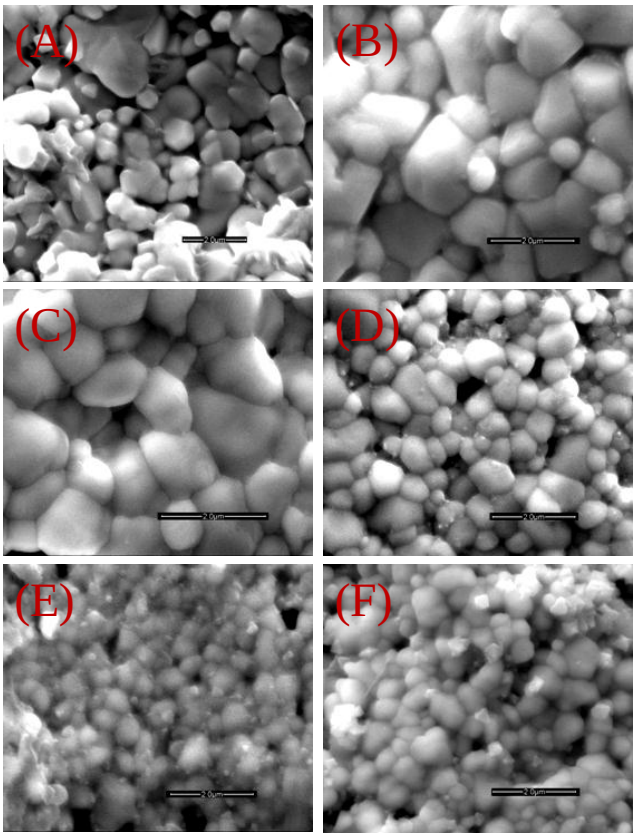

Fig. 4. SEM micrograph of PYZT, (A) *x* = 0.00, (B) *x* = 0.02, (C) *x* = 0.04, (D) *x* = 0.06, (E) *x* = 0.08, (F) *x* = 0.10.

Microstructural analysis

The surface grain distribution of pure and yttrium doped PZT (65/35) is shown in **Fig 4**. All the samples have uniform grain distribution with reasonable porosity. The edges of the grains were not sharp as yttrium doping increases, which may be due to melting nature of the sample. Thus yttrium doping optimized the sintering

conditions of PZT. The average grain size was calculated by classical least interception method and the grain size data is presented in **Table 1** as a function of *Y* doping. From the data it is found that grain size decreases with *Y* doping except at $x = 0.10$. The Y^{3+} ion occupies Pb^{2+} site in the ABO_3 unit cell, as a result to achieve charge neutrality Y^{3+} at A site generates lead vacancies, which may further result to decrease in grain size with *Y* doping. The porosity calculations further supports this argument. Sintered pellets were grinded and the apparent density (ρ_a) of powders was determined using Archimedes's technique, further theoretical density (ρ_t) was calculated and the percentage of porosity was determined using the **Equ. 1**. The porosity data shown in the **Table 1** suggests that, the porosity increases with increasing *Y* doping except at $x = 0.10$. This observation suggests that *Y* doping generates lead vacancies in the PZT ceramic.

$$\%Porosity = \left(1 - \frac{\rho_a}{\rho_t}\right) X100 \quad \text{---------- (1)}$$

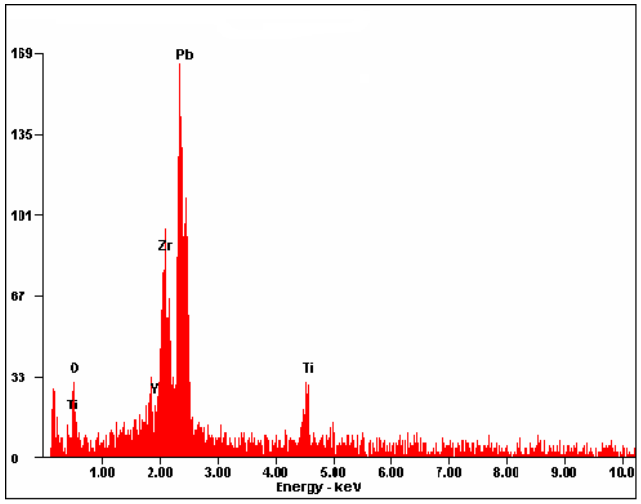

Fig. 5. The results of EDAX analysis performed on PYZT (65/35), $x = 0.04$ sample.

Elemental analysis

Fig. 5 shows the EDAX spectrum of *Y* doped PZT (65/35), $x = 0.04$ sample, the energy peaks identified are found to belong to the individual elements present in the compound. The EDAX spectrum was taken at five different positions of each sample and the average atomic percentage (logarithmic change) of each element as a function of *Y* doping is shown in the **Fig. 6**. From the figure it is found that zirconium was the only element found to have constant atomic percentage, throughout the *Y* doping upto $x = 0.10$ in PZT (65/35). The lead atomic percentage was found to decreasing and *Y* atomic percentage was found to increase continuously as we move from left to right of graph, which is expected, because we are substituting *Y* at *Pb* site itself. So as the *Y* doping increased the atomic percentage of *Y* increases and *Pb* decreases. However by close observation of Titanium atomic percentage we see that, upto $x = 0.04$ *Y* occupied at *A* site replacing *Pb* and beyond this limit, it occupied both *A* and *B* site replacing *Pb* and *Ti* respectively and hence this may be the reason for the decrease in *Ti* atomic percentage beyond x = 0.04.

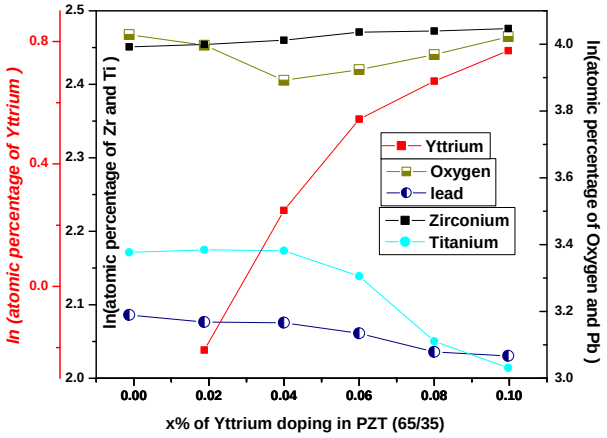

Fig. 6. Variation of atomic percentage of different elements of PYZT, drawn from EDAX results.

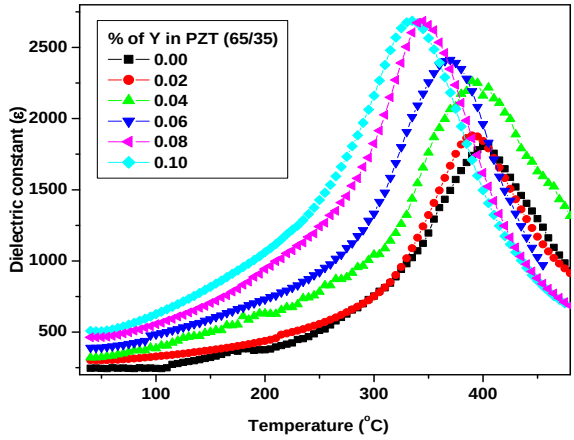

Fig. 7. Variation of dielectric constant as function of temperature for various *Y* doped PZT (65/35) compositions at 1 kHz.

Electrical property analysis

Fig. 7 shows the variation of dielectric constant as a function of temperature at various *Y* doping in PZT (65/35) composition, all the compositions show normal dielectric behavior of increase up to phase transition temperature T_C and then decrease beyond it. The maximum dielectric constant was found to increase with *Y* doping and T_C was found to shift towards lower temperature. The decrease in T_C was expected to be due to decrease in unit cell parameters, and hence the volume of unit cell decreases, as a result dipole moment decreases, which may further result to decrease in T_C. The ferroelectric hysteresis loop of *Y* doped PZT (65/35) at 20 kv/cm applied field is shown in the **Fig. 8**. The remnant polarization P_r was found to increase with Y doping, where as coercivity E_C was found to increase upto $x = 0.04$ and then found to decrease with *Y* doping. Our results are better than the reported [**9**] for thin films of PZT (52/48) +2% Y doping and $Pb(Zr_{0.40}\ Ti_{0.60})O_3$

(Y-PZT) [**10**]. The reported P_s = 40 (μC/cm^2), P_r = 26 (μC/cm^2), E_c = 160 kV/cm and ε_r = 2100 in [**9**] and P_r = 40 (μC/cm^2) in [**10**] are inferior to our achieved value of P_s = 68 (μC/cm^2), P_r = 43.9 (μC/cm^2), E_c = 10 kV/cm and ε_r = 2687 for $Pb_{0.9}Y_{0.1}(Zr_{0.65}Ti_{0.35})O_3$ (i.e., x = 0.10). All these observations suggest, *Y* doped PZT (65/35) is one of the best promising material which shows excellent ferroelectric and dielectric properties.

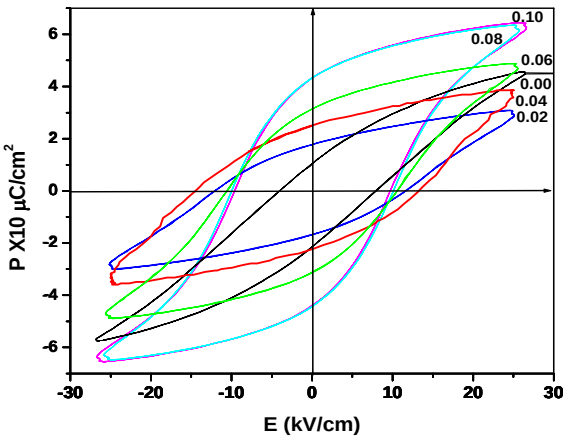

Fig. 8. P-E loop of different *Y* doped PZT (65/35) compositions.

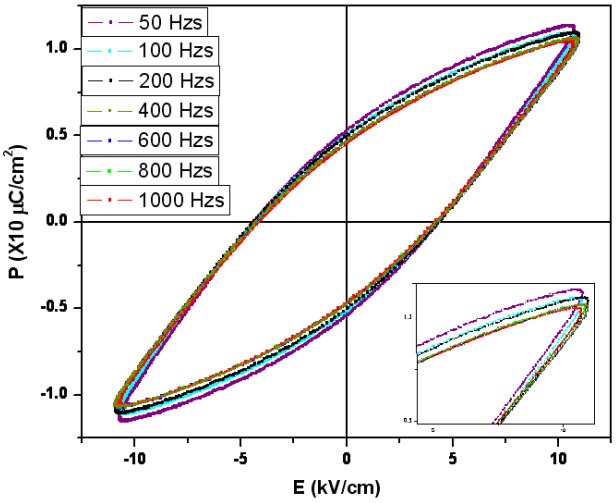

Fig. 9. P-E loop of PYZT (65/35), x = 0.10 composition at various measured frequencies.

Further frequency dependent conductivity was studied from P-E loop measurements. **Fig. 9** shows the P-E loop of PYZT, x = 10 taken at 0.8kV/cm measured at different frequencies, starting from 50Hz to 1 kHz. The inset of the figure is the magnified image of right top part of same P-E loop, to show the saturation magnetization variation with measured frequency. It is clear from the inset figure that, the saturation found to decrease with increasing measured frequency. That is as the applied frequency increased, the loop gets unsaturated. This is because as the frequency increases, the conducting nature of the sample increases, and hence loop gets unsaturated at higher frequencies.

Conclusion

Yttrium doped lead zirconium titanate (PYZT) was prepared by chemical route of co-precipitation techniques using their nitrate salts. X-ray diffraction results confirm the formation of single rhombohedral phase for the samples calcined at 750 ^{o}C. No additional peak found in XRD confirms the complete solubility of *Y* up to x = 0.10 limit. A uniform surface grain distribution with decreasing grain size was found with *Y* doping. The dielectric maxima was found to be enormously increased from 1791 to 2687 along with decreasing phase transition temperature from 335 to 400 ^{o}C with *Y* doping in PZT. The remnant polarization was also found to increase from 11 to 43.9 μC/cm^2 with *Y* doping where as coercivity E_C was found to increase up to x = 0.04 and then found to decrease with *Y* doping. All these observations suggest, *Y* doped PZT (65/35) is one of the best promising material which shows excellent ferroelectric and dielectric properties.

Acknowledgement

K.L.Y thanks to Council of Scientific and Industrial Research, New Delhi, India for financial support under the project grant number 03(1156/10/EMR-II).

References

1. Paiva-Santos, C.O.; Oliveira, C.F.; Las, W.C.; Zaghete, M.A.; Varela, J.A.; Cilense, M. *Mater. Res. Bull.* **2000**, *35*, 15.
2. Dai, X.; Xu, Z.; Viehland, D. *J. Am. Ceram. Soc.* **1995**, *78*, 2815.
3. Kakegawa, K.; Mohri, J.; Takahashi, T.H.; Shirasaki, S. *Solid State Commun.* **1977**, *28*, 769.
4. Scott, J.F.; Kammerdimer, L.; Parris, M.; Trayner, S.; Ottenbacher, V.; Shawabke, A.; Oliver, W.F. *J. Appl. Phys.* **1988**, *64*, 787.
5. Okuyama, M.; Matsui, Y.; Nakamo, H.; Hamakawa, Y. *Ferroelectrics* **1981**, *33*, 235.
6. Wu, S.Y.; Takei, W.J.; Francobe, M.H. *Ferroelectrics* **1976**, *10*, 209.
7. Thomas, R.; Mochizuki, S.; Mihara, T.; Ishida, T. *Thin Solid Films* **2003**, *443*, 14.
8. Yoshikawa, Y.; Tsuzuki, K.; Kobayashi, T.; Takagi, A. *J. Mater. Sci.* **1988**, 23, 2729.
9. Dalakoti, A.; Bandyopadhyay, A.; Bose, S. *J. Am. Ceram. Soc.* **2006**, *89*, 1140.
10. Cheng, W.X.; Ding, A.L.; Qiu, P.; He, X.; Zheng, X. *Integrated Ferroelectrics* **2005**, *75*, 173.

